Eurographics Workshop on Visual Computing for Biology and Medicine (2016)
H. Hauser, A. Hennemuth, and A. Lundervold (Editors)

Short Paper

Semi-Automatic Vessel Boundary Detection in Cardiac 4D PC-MRI Data Using FTLE fields

B. Behrendt[1], B. Köhler[1], D. Gräfe[2], M. Grothoff[2], M. Gutberlet[2] and B. Preim[1]

[1]Dept. of Simulation and Graphics, University of Magdeburg, Germany
[2]Dept. of Diagnostic and Interventional Radiology, Herzzentrum Leipzig, Germany

Abstract

Four-dimensional phase-contrast magnetic resonance imaging (4D PC-MRI) is a method to non-invasively acquire in-vivo blood flow, e.g. in the aorta. It produces three-dimensional, time-resolved datasets containing both flow speed and direction for each voxel. In order to perform qualitative and quantitative data analysis on these datasets, a vessel segmentation is often required. These segmentations are mostly performed manually or semi-automatically, based on three-dimensional intensity images containing the maximal flow speed over all time steps. To allow for a faster segmentation, we propose a method that, in addition to intensity, incorporates the flow trajectories into the segmentation process.
This is accomplished by extracting Lagrangian Coherent Structures (LCS) from the flow data, which indicate physical boundaries in a dynamical system. To approximate LCS in our discrete images, we employ Finite Time Lyapunov Exponent (FTLE) fields to quantify the rate of separation of neighboring flow trajectories. LCS appear as ridges or valleys in FTLE images, indicating the presence of either a flow structure boundary or physical boundary. We will show that the process of segmenting low-contrast 4D PC-MRI datasets can be simplified by using the generated FLTE data in combination with intensity images.

Categories and Subject Descriptors (according to ACM CCS): I.4.3 [Computer Graphics]: Filtering—FTLE

1. Introduction

Various cardiovascular pathologies have been related to changes in blood flow patterns [HSD13]. To gain a better understanding of these pathologies, analyzing their respective patterns is vital. With four-dimensional phase-contrast magnetic resonance imaging *(4D PC-MRI)*, it is possible to non-invasively obtain patient-specific blood flow data. A segmentation of the datasets is often needed to find seeding points for pathlines and quantify various measures, such as stroke volumes and regurgitation fractions [KPG*16b].

Commonly, segmentations are carried out manually or semi-automatically based on the dataset's magnitude values, e.g. using the temporal maximum intensity projection (*TMIP*), which depicts the maximum flow speed over all time steps [KBP*15]. Methods range from simple thresholding [BKPP16] to more sophisticated methods like Active Contours [KULD08] or Graph Cuts [KPG*16a]. A purely TMIP-based approach is sufficient for images with good overall contrast, (Fig. 1(a)), but becomes cumbersome on datasets with lower contrast (Fig. 1(b) and (c)). Since in such cases the differences in local contrast make the TMIP images unsuitable to base a segmentation on, we propose the additional usage of directional information. Flow inside of a blood vessel generally follows the vessel's course, while movement perceived outside consists mostly of random noise. Therefore, the presence of a general flow direction distinguishes the vessel anatomy from their surroundings. This distinction can provide additional valuable information for segmentation purposes.

A way of quantifying this distinction is the Finite Time Lyapunov Exponent (*FTLE*) [Hal02], which is a measure of the rate of separation of infinitesimally close trajectories in a specified time frame of a dynamic system. The lack of coherent flow outside of the anatomy results in a high rate of separation in the direct vicinity of the vessel boundary, as this is where directed flow borders on random motion. Therefore, areas of high intensity in an FTLE image can be interpreted as an approximation of the vessel boundary [KGG*12].

This paper presents an algorithm which incorporates directional coherency information through the use of FTLE fields in addition to TMIP-based images. We will show that the segmentation process can be significantly sped up in comparison to classical methods based solely on magnitude.

2. Related Work

In this section, we will give an overview of the use of FTLE in flow data to identify structures and briefly discuss alternative methods of using directional information for segmentation purposes.

An example for a different flow coherency measure is the Local

DOI: 10.2312/vcbm.20161269

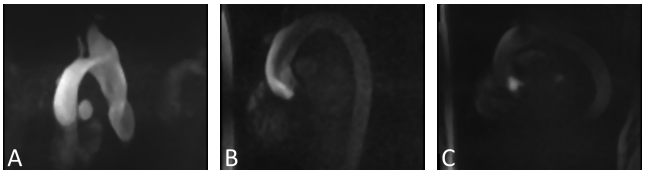

Figure 1: Comparison of TMIP image slices showing the aorta with different contrast levels. The first image can easily be segmented on image intensity alone; the second and third one suffer from low contrast in the aortic arch and descending aorta.

Phase Coherence (*LPC*), as proposed by Chung et al. [CNS04]. It is defined as the sum of dot products of a voxel's flow vector with those of the adjacent vectors, so coherent flow in a blood vessel generates higher LPC values than the surrounding random noise. In studies with clinical data, Chung et al. proved that the use of LPC for segmentation is less error-prone when there is a low signal-to-noise ratio (*SNR*). However, on datasets with high SNR, segmentations on magnitude images outperformed those on LPC images.

The LPC only takes into consideration the flow of single time steps and is therefore susceptible to noise. This can be partly remedied by averaging LPCs over all time steps. FTLEs, on the other hand, incorporate flow information over multiple time steps. A general approach to visualize complex structures from arbitrary flow fields using FLTEs was presented by Ferstl et al. [FBTW10]. They simulated flow around simple, geometric obstacles and employed the ridges of FTLE fields as seeding points for streak surfaces.

Van Leeuwen used FTLE fields as basis for clustering intracardiac blood flow acquired using 4D PC-MRI [vL14]. This was done to focus the complex visualization on important flow structures by partitioning the presented information and removing visual clutter. Instead of focusing on inset flow structures, Krishnan et al. introduced an algorithm for boundary detection of an entire vessel, albeit not for the purpose of segmentation [KGG*12]. They used high FTLE values as a stopping criteria for their pathline integration in order to prevent them from leaking out of the vessel anatomy. However, the absence of an actual segmentation requires manual placing of seed points and prevents native support for visualizing parameters of the aortic wall, such as wall shear stress.

3. Background

Four-dimensional phase-contrast magnetic resonance imaging *(4D PC-MRI)* is an imaging modality that allows for a non-invasive acquisition of three-dimensional time-resolved blood flow data from a patient. This information helps finding correlations between various pathologies and changes in blood flow patterns, allowing for a better understanding of cardiovascular diseases.

3.1. Data Acquisition and Preprocessing

Data acquired using 4D PC-MRI consists of 3 flow images representing direction and 3 magnitude images representing speed for each slice and time step. From these images, a four-dimensional velocity vector field can be constructed.

The acquisition requires a velocity encoding parameter (V_{enc}), denoting the highest expected velocity for each direction [SAG*14]. If the actual flow velocity exceeds the preset V_{enc}, it flips and therefore appears to be moving in the opposite direction. These artifacts are called *phase wraps* and appear either as white areas surrounded by black or black areas surrounded by white in the resulting datasets.

Using a high V_{enc}, on the other hand, lowers the overall image contrast and therefore increases the difficulty of segmenting the anatomy. A similar problem can occur if the vessel simultaneously has areas of very high (e.g. inflow jets) and low (e.g. parts of the aortic arch) flow speed, which is often the case in clinically interesting pathologic datasets. Here, the V_{enc} has to be increased in order to prevent phase wrapping artifacts in certain regions, therefore lowering contrast in others (Fig. 1(b) and (c)). Thus, low quality data is not a matter of wrong adjustments of inexperienced users.

3.2. Lagrangian Coherent Structures

Lagrangian Coherent Structures (*LCS*) are trajectory structures in a dynamical system that indicate the presence of physical boundaries or other major influences on the flow [SLM05]. These structures can be approximated by calculating the Finite Time Lyapunov Exponent (*FTLE*) of every voxel in a dataset. In the resulting FTLE field, LCS appear as ridges.

The base for an FTLE field calculation is the dataset's flow map $\Phi_t^{t+\delta t}(v)$ [SDM06]. It maps each voxel $v = (x,y,z)$ in the four-dimensional dataset to the position, a massless particle integrated from v at time step t would have at the time point $t+\delta t$. Parameters of this process are step size, integration time δt and integration method. The step size controls the number of sampling points for the integration process. Increasing the step size can increase the calculation speed at the cost of accuracy. The optimal integration time varies with each dataset, as it is dependent on variables like overall flow speed and turbulences [vL14].

In areas with coherent flow, neighboring voxels in the flow map should reach a similar final integration position. Due to the coherent flow of the vessel in contrast to the random noise outside, the aorta's shape is clearly distinct in this image.

$$J(v,t,\delta t) = \nabla \Phi_t^{t+\delta t}(v) \tag{1}$$

$$\lambda(v,t,\delta t) = \sqrt{\lambda_{max}(J(v,t,\delta t)^T J(v,t,\delta t))} \tag{2}$$

$$FTLE(v,t,\delta t) = \frac{1}{|\delta t|}\log(\lambda(v,t,\delta t)) \tag{3}$$

To obtain the actual FTLE value of each voxel v at time t (Eq. 3), its spatial gradient or Jacobian $J(v,t,\delta t)$ is needed [KGG*12]. It represents the separation of flow around v in all directions and can be quantified as a single, scalar value by calculating its Euclidean or Spectral norm. λ_{max} in Eq. 2 is the maximum eigenvalue of the matrix $J^T J$. The logarithm in Eq. 3 is applied to account for the exponential growth of this term. Additionally, its numerical stability towards changes of the integration time δt is increased by performing a normalization [KGG*12].

4. Segmentation of Vessel Boundaries

Most applications for the quantification of four-dimensional cardiac blood flow require a segmentation of the vessel anatomy. While the segmentation can be mostly automated on datasets with good overall contrast [BKPP16], manually segmenting lower quality images is often cumbersome. Hennemuth et al. proposed the use of an interactive watershed transformation for image segmentation [HFS*11], using include and exclude markers in regions separated by watersheds to generate a segmentation. A similar segmentation input is used by interactive graph cuts, introduced by Boykov et al. [BJ01]. They employ both soft constraints based, for instance, on intensity and gradients, as well as hard constraints. The latter are regions manually marked by the user as either being part of the fore- or background. Images are interpreted as a graph, whereas neighboring pixels are connected via an edge that is weighted according to the soft constraints. By finding a cut of the graph, where the manually marked pixels are completely separated and costs of the cut edges are minimal, a segmentation can be achieved.

This approach offers users a fast, intuitive and stable way of segmenting the datasets. Physicians only need to apply their knowledge of the anatomy during the segmentation process, instead of having to adjust abstract parameters. Since vessel boundaries are naturally indicated by changes in the magnitude image intensity, their gradients usually are a suitable choice as soft constraints for weighting the edges. On images containing gradients of highly varying intensity due to local contrast differences, this most likely results in an unsatisfactory segmentation. In this paper, we will show that improving the soft constraint by adding information derived from flow images reduces the amount of interaction required by the user on low-contrast datasets.

4.1. Clinical Data

In order to test our approach, we used four clinical datasets showing the aorta and pulmonary artery of healthy volunteers as well as patients with different pathologies. Each dataset consists of six images with a grid resolution of $132 \times 192 \times 15$ - 26 for each of their 11 to 23 time steps, containing flow direction and magnitude in x, y and z direction. From the magnitude data, a temporal maximum intensity projection (*TMIP*) was created. The flow data was used to create a temporal standard deviation image (*STDEV*) [WCS*93] and a finite time Lyapunov exponent image (*FTLE*). To approximate the flow trajectory during the flow map calculation, we are using the 4th-order Runge-Kutta integration (*RK4*), with a step size of 1, which offers an acceptable compromise between accuracy and speed. Due to the absence of a heuristic to determine the optimal integration time before actually performing the integration, we opted for a fixed value of 20% of the dataset's overall time frame (100 - 120 ms). Since we are interested in the ridges of the FTLE image, a normalization above the 80% quantile was applied (Fig. 2(a) and (b)). To increase the contrast in our FTLE images, a TMIP was applied. As a measurement of flow separation, FTLEs are strongly dependent on the time frame they are generated over (defined by t and δt), so there is no need to calculate them over time frames without significant flow. Therefore, the diastolic phase can be skipped during FTLE calculation (Fig. 2(c)).

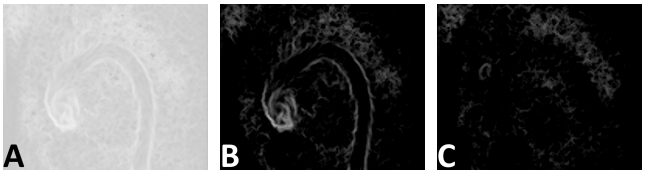

Figure 2: FTLE slice generated for a time frame over the systole with (b) and without (a) normalization above the 80% quantile, diastolic FTLE frame with normalization (c).

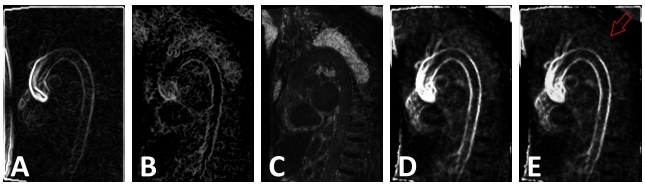

Figure 3: Slices from the input and output data; TMIP gradient (*a*), FTLE (*b*) and STDEV (*c*) input images. The last two images show the result with (*e*) and (*d*) including the STDEV image. The red arrow highlights an area, where including the STDEV reduces noise.

4.2. Vessel Boundary Enhancement

In addition to boundaries, certain inset flow structures can also cause high FTLE values. For instance, strong vortices or inflow jets can sometimes be hard to differentiate from the actual vessel boundaries (Fig. 3(b)). Also, FTLE images are sensitive to noise, which is likely to appear in air-filled areas. In order to increase the robustness of our approach against such structures, we use additional information from the TMIP and flow data to reduce or eliminate their effects.

Although the gradient of the TMIP images alone may not be sufficient to detect vessel boundaries (Fig. 3(a)), it can still help to rule out unwanted boundaries detected in the FTLE image. By normalizing both the TMIP gradient and FTLE image to an intensity range of 0 to 1 and multiplying them, we can enhance the contrast of the actual vessel boundary. In both the gradient and FTLE image, the actual boundary should have comparatively high values, while most inset flow structures are only visible in the FTLE image. This creates an image with high intensities on the vessel boundaries, but also a high amount of noise, especially in the lung (Fig. 3(d)). As proposed by Walker et al., we generated the STDEV image by adding up the flow's temporal standard deviation over all time steps for each voxel to remove these artifacts [WCS*93]. Areas with an exceptionally high standard deviation are most likely to be air-filled regions and therefore cannot be part of the vessel anatomy (Fig. 3(c)). They can therefore be filtered out by multiplying our image with the inverse of a normalized STDEV image. In the resulting image, which we will reference as Enhanced FTLE (*EFTLE*), vessel boundaries are clearly visible with minimal noise (Fig. 3(e)).

After acquiring and preprocessing the dataset, our application generates the necessary derived images like TMIP and flow map

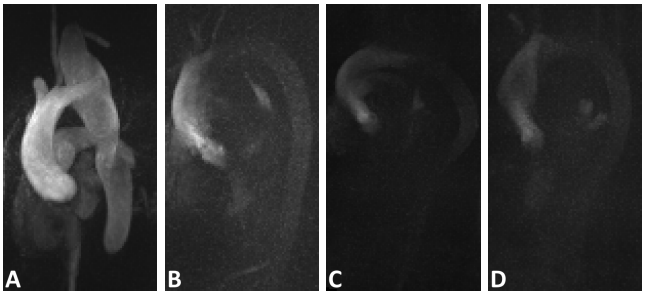

Figure 4: Datasets segmented by our expert radiologist; `ISTA_12_2012` (a), `Flow_DS_3_2014` (b), `Flow_DS_6_2014` (c), `Flow_DS_9_2014` (d).

using parallel processing on the GPU. Generating the flow map takes the most time, as it requires to integrate the flow for each voxel in every time step. The actual segmentation is performed using the 3D graph cut implementation GridCut, with edge weights specified by the function $e^{-\alpha \cdot ||\nabla I||^2}$. I is the image intensity and α a tolerance parameter with an experimentally determined value of 1000 [KPG*16a]. The user has to manually classify small regions using a paint brush tool as belonging to either the vessel anatomy (green) or background (red) [KPG*16a]. At any time, the user can generate the 3D surface mesh from the segmentation to identify and correct regions with segmentation errors.

5. Evaluation

To evaluate our method, we asked an expert radiologist to use it as a base to segment four datasets (Fig. 4), which were selected as representations of different contrast levels. The radiologist segmented all datasets twice, once based on TMIP and once on EFTLE images. To objectively evaluate our approach against classical methods, we compared both required input for and resulting vessel model from both segmentations.

The quantification of user input consists of counting how many voxels the radiologist had to manually color in order to reach a satisfying segmentation. In order to make the results comparable between different datasets with varying resolutions and vessel volumes, we calculated the ratio of manually segmented voxels in TMIP and EFTLE images. To ascertain that the user input for segmenting the EFTLE images would not also generate a good segmentation on a TMIP, the input for both EFTLE- and TMIP-based segmentations was then reapplied to the other image. We also applied EFTLE-based input to LPC images and compared the resulting segmentations to evaluate our method against the Local Phase Coherency (*LPC*) by Chung et al.

6. Results

All preprocessing tasks were performed before the radiologist started segmenting the images. On a *Geforce GTX980*, generating a flow map without the diastolic time frame took around 1 to 3 min., depending on the dataset dimensions. During an informal interview, the radiologist expressed that especially for the datasets with poor

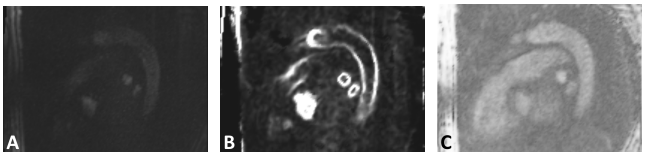

Figure 5: A slice rendered as TMIP (a), EFTLE (b) and LPC (c).

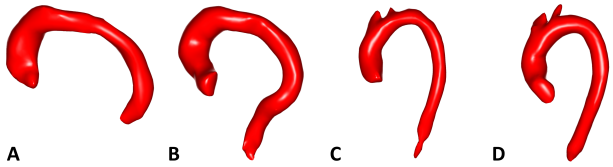

Figure 6: Vessel mesh extracted from the segmentation of `Flow_DS_6_2014` (a, b) and `Flow_DS_3_2014` (c, d); the vessels generated from a magnitude-based segmentation (a, c) cover less of the anatomy than those generated from our method (b, d).

contrast, EFTLE images were much easier to segment because the anatomy was much clearer to see (Fig. 5(b)). The TMIP-based segmentation of the dataset in Fig. 6(a) is missing parts of the descending aorta that were not sufficiently visible in the magnitude images. In Fig. 6(c), the radiologist was unable to segment parts of the ascending aorta around the left ventricle. Both of these areas were made possible to segment using EFTLE images (Fig. 6(b) and (d)). Additionally, Fig. 6(d) shows a better segmentation of the vessels branching from the aortic arch, which are important landmarks in many applications. A reoccurring problem with segmenting EFTLE images is that the segmentation can leak from the aorta onto the pulmonary artery, since the graph cut has problems separating them in some areas. On the low-contrast datasets, however, the effort to manually correct these errors was significantly lower than the effort to create a magnitude-based segmentation.

Fig. 7 shows an overview of the ratio of foreground, background and overall manual segmentations. Due to the lack of a gold standard for the segmentations, we did not compute similarity measures such as the DICE coefficient. The two images with better contrast exhibit higher ratios, showing that our method was less efficient on them. Due to the aforementioned leaking of the segmentation into the pulmonary artery, `ISTA_12_2012` has an exceptionally high ratio for manually marked background voxels. On images with lower contrast levels, our approach performs significantly better, as it reduces the amount of required manual input by 22 to 32 percent.

Additionally, we applied the segmentation input for EFTLE images to TMIP images and in reverse. On datasets with better contrast, exchanging the input produced mostly valid segmentations in both cases. Applying the EFTLE input to TMIP images generally causes smaller areas to disappear from the resulting segmentation. In the reverse case, additional undesired areas belonging to the pulmonary artery become visible. The same things happen on the datasets with lower quality, although the effects are strongly increased. Applying the EFTLE input to TMIP images fails to produce a valid segmentation, because there is too little input for the

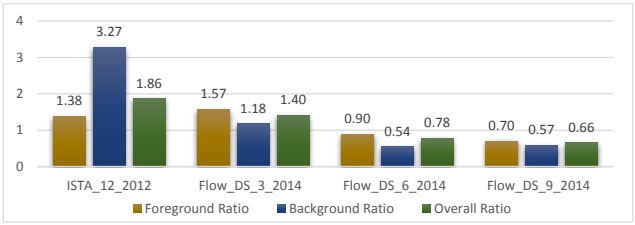

Figure 7: Ratios of manual segmentation input by our expert radiologist

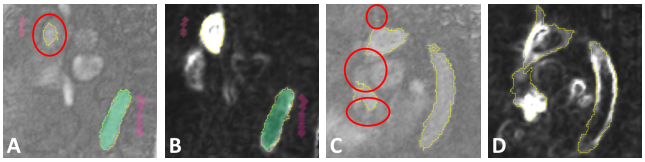

Figure 8: Comparison between LPC- and EFTLE-based segmentations (yellow outline) using the same input; Red circles in the LPC images (b, d) indicate areas with incomplete segmentation compared to EFTLE images (a, c).

graph cut to work with. This had to be solved by marking additional voxels as background, which still results in an unsatisfactory segmentation. Applying EFTLE input to LPC images produced a seemingly valid segmentation for all four datasets. On closer inspection, however, the vessel segmentation turned out to be incomplete. The graph cut algorithm fails to automatically include many voxels near the vessel boundary, likely due to generally lower SNR of LPC images (Fig. 8).

7. Conclusion and Future Work

In this paper, we presented a method to aid the segmentation of vessels in low-contrast cardiac 4D PC-MRI datasets. This was achieved by combining magnitude-based images with flow coherency information extracted from FTLE fields. Although we only tested it with cardiac 4D PC-MRI data, our method should be easily adaptable for other regions of the human body, as long as the vessels are large enough to be visible through 4D PC-MRI. Similarly to LPC, the resulting EFTLE images allow for a segmentation of the vessel even in areas with magnitude contrast or low signal-to-noise ratio. With the help of an expert radiologist we were able to confirm that our approach requires less input to generate a satisfying segmentation than an LPC-based method. While our approach works better on low-quality images, using the TMIP as a base for segmentation was preferable on high-contrast datasets. Therefore users should be able to switch between these two options, depending on the quality of their datasets. This may be remedied by a more detailed exploration of the algorithm's parameter space, namely the step size, integration time and scale of the FTLE image. Further studies need to be conducted in order to find a heuristic for determining optimal parameters for each dataset.

References

[BJ01] BOYKOV Y. Y., JOLLY M.-P.: Interactive graph cuts for optimal boundary & region segmentation of objects in N-D images. In *Proc IEEE Int Conf Comput Vis* (2001), pp. 105–112. 3

[BKPP16] BEHRENDT B., KÖHLER B., PREIM U., PREIM B.: Enhancing visibility of blood flow in volume rendered cardiac 4D PC-MRI data. In *Bildverarbeitung für die Medizin 2016* (2016), Springer, pp. 188–193. 1, 3

[CNS04] CHUNG A. C. S., NOBLE J. A., SUMMERS P.: Vascular segmentation of phase contrast magnetic resonance angiograms based on statistical mixture modeling and local phase coherence. *IEEE Trans Med Imaging 23*, 12 (2004), 1490–1507. 2

[FBTW10] FERSTL F., BURGER K., THEISEL H., WESTERMANN R.: Interactive separating streak surfaces. *IEEE Trans Vis Comput Graph 16*, 6 (2010), 1569–1577. 2

[Hal02] HALLER G.: Lagrangian coherent structures from approximate velocity data. *Physics of Fluids 14*, 6 (2002), 1851. 1

[HFS*11] HENNEMUTH A., FRIMAN O., SCHUMANN C., BOCK J., DREXL J., HUELLEBRAND M., MARKL M., PEITGEN H.-O.: Fast interactive exploration of 4D MRI flow data. In *SPIE Medical Imaging* (2011), SPIE Proceedings, SPIE, p. 79640E. 3

[HSD13] HOPE M. D., SEDLIC T., DYVERFELDT P.: Cardiothoracic magnetic resonance flow imaging. *J Thorac Imaging 28*, 4 (2013), 217–230. 1

[KBP*15] KÖHLER B., BORN S., PELT, ROY F. P. VAN, PREIM U., PREIM B.: A Survey of Cardiac 4D PC-MRI Data Processing. In *Eurographics Workshop on Visual Computing for Biology and Medicine* (2015), The Eurographics Association. 1

[KGG*12] KRISHNAN H., GARTH C., GUHRING J., GULSUN M. A., GREISER A., JOY K. I.: Analysis of time-dependent flow-sensitive PC-MRI data. *IEEE Trans Vis Comput Graph 18*, 6 (2012), 966–977. 1, 2

[KPG*16a] KÖHLER B., PREIM U., GROTHOFF M., GUTBERLET M., FISCHBACH K., PREIM B.: Motion-aware stroke volume quantification in 4D PC-MRI data of the human aorta. *Int J Comput Assist Radiol Surg 11*, 2 (2016), 169–179. 1, 4

[KPG*16b] KÖHLER B., PREIM U., GROTHOFF M., GUTBERLET M., FISCHBACH K., PREIM B.: Robust Cardiac Function Assessment in 4D PC-MRI Data of the Aorta and Pulmonary Artery. *Comput Graph Forum 35*, 1 (2016), 32–43. 1

[KULD08] KAINMULLER D., UNTERHINNINGHOFEN R., LEY S., DILLMANN R.: Level set segmentation of the heart from 4D phase contrast MRI. In *Medical Imaging* (2008), p. 691414. 1

[SAG*14] STANKOVIC Z., ALLEN B. D., GARCIA J., JARVIS K. B., MARKL M.: 4D flow imaging with MRI. *Cardiovascular diagnosis and therapy 4*, 2 (2014), 173–192. 2

[SDM06] SHADDEN S. C., DABIRI J. O., MARSDEN J. E.: Lagrangian analysis of fluid transport in empirical vortex ring flows. *Physics of Fluids 18*, 4 (2006), 047105. 2

[SLM05] SHADDEN S. C., LEKIEN F., MARSDEN J. E.: Definition and properties of Lagrangian coherent structures from finite-time Lyapunov exponents in two-dimensional aperiodic flows. *Physica D: Nonlinear Phenomena 212*, 3-4 (2005), 271–304. 2

[vL14] VAN LEEUWEN C.: *Spatial-temporal pathline clustering based on FTLE fields*. Master's Thesis, Delft University of Technology, Delft, 2014. 2

[WCS*93] WALKER P. G., CRANNEY G. B., SCHEIDEGGER M. B., WASELESKI G., POHOST G. M., YOGANATHAN A. P.: Semiautomated method for noise reduction and background phase error correction in MR phase velocity data. *J Magn Reson Imaging 3*, 3 (1993), 521–530. 3